GeoEdu Insight Journal: Geography and Education Geography
Vol. 1, No. 2, October 2026, pp. 162~178
ISSN: 3163-9070, DOI: 10.37251/gedij.v1i2.3983

Integrating Landsat 8 Imagery and GIS-Based Multi-Parameter Analysis for Regional Landslide Susceptibility Mapping in South Central Timor, Indonesia

Jundri Simson Ati[1], Philip Baidoo[2], Sizakele Matilda Serame[3]
[1]Department of Geodesy Engineering, Faculty of Civil Engineering and Planning, Institut Teknologi Nasional Malang, Malang, Indonesia
[2]Faculty of Social Sciences Education (FSSE), Department of Geography Education, University of Education-Winneba, Winneba, Ghana
[3]Department of Geography and Environmental Science, University of Fort Hare, Eastern Cape Province, South Africa

Article Info

Article history:

Received Jul 30, 2026
Revised Aug 27, 2026
Accepted Oct 23, 2026
Online First Oct 31, 2026

Keywords:

Geographic Information Systems
Landsat 8
Landslide Susceptibility
Maximum Likelihood
Spatial Overlay

ABSTRACT

Purpose of the study: This study aims to identify and analyze the spatial distribution of landslide susceptibility in South Central Timor Regency, East Nusa Tenggara, Indonesia, using Landsat 8 imagery and Geographic Information Systems (GIS) by integrating land cover, rainfall, slope, and soil type parameters.

Methodology: This study employed quantitative spatial analysis using Landsat 8 imagery acquired in 2014 with a spatial resolution of 30 m. Land-cover classification was performed using the supervised Maximum Likelihood method in ENVI 5.1. Spatial processing, parameter scoring, and overlay analysis were conducted using ArcGIS 10.1. Field verification utilized a Garmin 76CSx GPS receiver and photographic documentation.

Main Findings: The analysis identified five landslide susceptibility classes. Moderate susceptibility was dominant, covering 293,501.038 ha (74.35%), followed by high susceptibility at 53,978.392 ha (13.67%), low susceptibility at 38,851.323 ha (9.84%), and non-susceptible areas at 8,229.700 ha (2.08%). Very high susceptibility covered 198.596 ha (0.05%). Land-cover classification achieved 96.0726% overall accuracy.

Novelty/Originality of this study: The study provides a regional geospatial assessment of landslide susceptibility by integrating Landsat 8-derived land-cover information with rainfall, slope, and soil-type parameters in South Central Timor Regency. Its contribution lies in presenting susceptibility patterns at both regency and district levels, providing spatial information that can support preliminary identification, regional planning, and prioritization of further field investigations.

This is an open access article under the CC BY license

Corresponding Author:
Jundri Simson Ati,
Department of Geodesy Engineering, Faculty of Civil Engineering and Planning, Institut Teknologi Nasional Malang,
Jl. Bendungan Sigura-gura No. 2, Malang 65145, East Java, Indonesia
Email: jundrisimsonati11@gmail.com

1. INTRODUCTION

Landslides are among the most significant natural hazards in mountainous and hilly regions, potentially causing substantial damage to infrastructure, settlements, and the surrounding environment. The occurrence of landslides is influenced by various interacting environmental factors, including slope characteristics, rainfall, soil

properties, and land cover [1]-[3]. Identifying areas that are potentially susceptible to landslides is therefore essential for supporting disaster risk reduction and spatial planning [4]-[6]. Remote sensing and Geographic Information Systems (GIS) provide valuable approaches for identifying and analyzing spatial variations in landslide susceptibility [7]-[9]. Satellite imagery, particularly Landsat 8, offers multispectral information that can be used to identify land-cover characteristics, while GIS enables the integration and spatial analysis of multiple thematic datasets [10]-[12]. These capabilities are particularly relevant to South Central Timor Regency, East Nusa Tenggara, Indonesia, where variations in topography and environmental conditions require spatially based approaches to landslide-prone area identification.

The identification of landslide-prone areas requires the consideration of several environmental parameters that may contribute to slope instability. However, these parameters are often available in different spatial datasets and formats, making their integration and analysis challenging. Land-cover conditions influence surface characteristics and human activities, while slope gradient affects the stability of hillsides [9], [13], [14]. Rainfall can act as a triggering factor by increasing soil moisture and reducing soil strength, whereas soil type is associated with the physical and mechanical properties of the ground [15]-[17]. An analysis based on only one parameter may therefore be insufficient to describe the spatial variation of landslide susceptibility [18]-[20]. Integrating land cover, slope, rainfall, and soil type within a GIS environment provides a more comprehensive basis for identifying areas with different levels of potential landslide susceptibility.

This study employs Landsat 8 imagery and GIS-based spatial analysis to identify areas potentially susceptible to landslides in South Central Timor Regency. Landsat 8 imagery is processed using supervised classification with the Maximum Likelihood method to generate land-cover information [21], [22]. The resulting land-cover data are then integrated with slope, rainfall, and soil-type datasets [23], [24]. Each parameter is assigned a score according to its contribution to landslide susceptibility, and the scoring results are combined through spatial overlay analysis [25], [26]. The final analysis produces five susceptibility classes: non-susceptible, low, moderate, high, and very high [27], [28]. This approach provides a spatial representation of the distribution of landslide susceptibility based on the integration of multiple environmental parameters.

Previous studies have demonstrated the potential of remote sensing, GIS, and multi-criteria approaches for landslide susceptibility assessment. Devara et al. [29] integrated MT-InSAR and the Analytical Hierarchy Process (AHP) within a GIS-based multi-criteria decision analysis framework to assess landslide susceptibility. Lima et al. [30], through a review and bibliometric analysis of data-driven landslide susceptibility assessment, highlighted the development of statistical and machine-learning approaches, as well as the importance of model validation. Ibrahim et al. [31] examined advanced data-mining techniques for landslide susceptibility mapping, demonstrating the application of approaches such as Naïve Bayes and Random Trees. More recently, Sharma et al. [32] developed high-resolution landslide susceptibility mapping using ensemble machine-learning techniques and geospatial big data. Ali et al. [33] investigated high-resolution landslide mapping and susceptibility assessment, including temporal variations in landslides and vegetation recovery. In addition, Ehsan et al. [34] reviewed geological and triggering factors influencing landslide susceptibility and identified the growing application of artificial intelligence in landslide mapping and prediction.

Although these studies have advanced landslide susceptibility assessment through multi-criteria analysis, data-driven modelling, and machine-learning techniques, the selection and integration of environmental parameters remain important considerations in regional-scale mapping. Different geographical areas may exhibit different combinations of terrain, soil, rainfall, and land-cover characteristics, requiring approaches that reflect local environmental conditions. In South Central Timor Regency, the integration of Landsat 8-derived land-cover information with slope, rainfall, and soil-type data provides an opportunity to examine the spatial distribution of landslide susceptibility. Accordingly, this study focuses on combining these four parameters through a scoring and overlay approach to produce a regional landslide susceptibility map. The emphasis is on the application of integrated geospatial analysis to the study area rather than the development of a new classification or prediction algorithm.

The contribution of this study lies in the integration of Landsat 8 imagery and GIS-based thematic parameters to identify landslide susceptibility levels in South Central Timor Regency. The use of supervised Maximum Likelihood classification provides land-cover information derived from satellite imagery, while the integration of slope, rainfall, and soil-type data enables the assessment of multiple environmental characteristics within a unified spatial framework. The resulting susceptibility map is expected to provide information on the distribution of areas classified as non-susceptible, low, moderate, high, and very high susceptibility. This regional application contributes to the use of remote sensing and GIS as supporting tools for environmental assessment and spatial identification of potential landslide-prone areas.

The assessment of landslide susceptibility is important for providing spatial information that can support disaster risk management and regional planning. Identifying areas with different levels of potential susceptibility can help stakeholders recognize locations that may require further attention, field investigation, and appropriate land-use considerations [35], [36]. Therefore, this study aims to utilize Landsat 8 imagery and Geographic Information Systems to identify and analyze the distribution of landslide susceptibility in South Central Timor

Regency by integrating land cover, slope, rainfall, and soil type through a scoring and spatial overlay method. The results are expected to provide a spatial basis for understanding the distribution of potential landslide-prone areas in the study region.

2. RESEARCH METHOD

2.1. Research Design and Study Area

This study employed a quantitative spatial analysis approach integrating remote sensing and Geographic Information Systems (GIS) to identify areas potentially susceptible to landslides [37], [38]. The study was conducted in Timor Tengah Selatan Regency, East Nusa Tenggara Province, Indonesia. The assessment integrated four environmental parameters, namely land cover, slope gradient, soil type, and rainfall. Landsat 8 imagery was used to derive land-cover information, while supporting thematic maps were processed and integrated through spatial overlay analysis. The final output was a landslide susceptibility map representing five susceptibility categories across the study area.

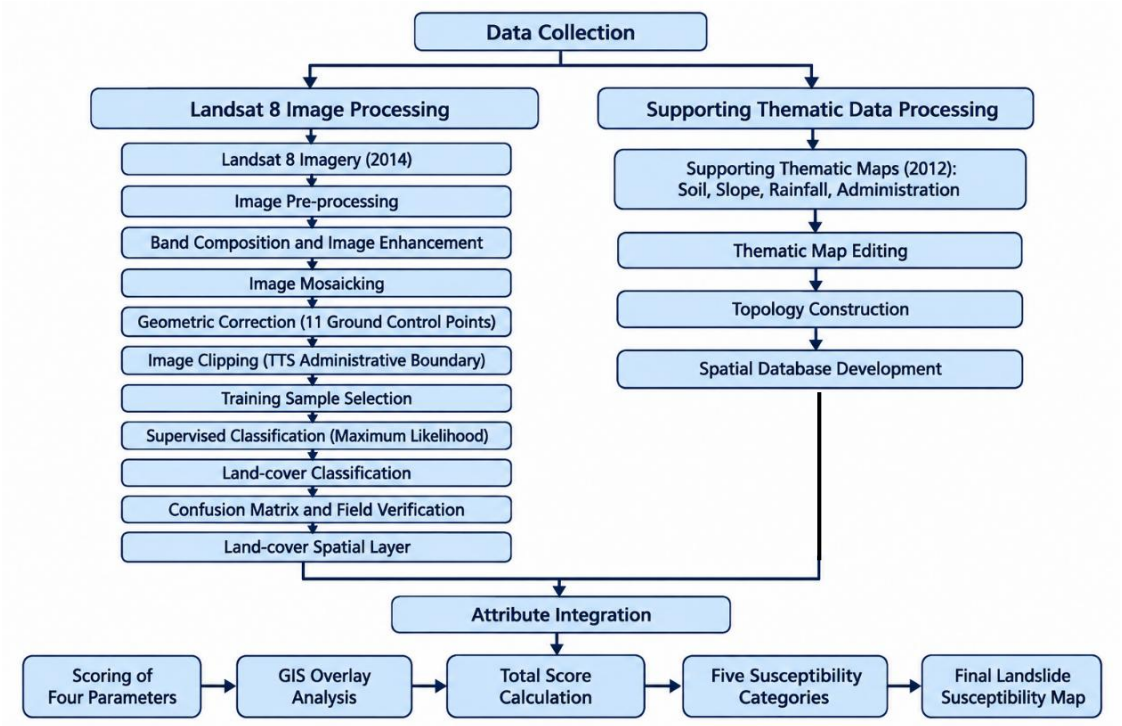


Figure 1. Research workflow for Landsat 8 image classification and GIS-based landslide susceptibility assessment in Timor Tengah Selatan Regency

2.2. Data Sources and Research Materials

The research utilized satellite imagery, thematic spatial datasets, and field observation data. Landsat 8 imagery acquired in 2014 was used as the primary source for land-cover classification. Supporting spatial datasets consisted of administrative boundaries, soil-type maps, slope maps, and rainfall maps, all at a scale of 1:250,000 and dated 2012. Field observations were conducted to examine the land-cover classification results using GPS coordinates and photographic documentation. The data sources, materials, and their respective analytical purposes are presented in Table 1.

Table 1. Data sources and materials used in the study

No.	Data	Year/Scale	Analytical purpose
1	Landsat 8 satellite imagery	2014	Land-cover classification
2	Administrative boundary map	2012; 1:250,000	Study-area delineation
3	Soil-type map	2012; 1:250,000	Soil susceptibility assessment
4	Slope map	2012; 1:250,000	Slope susceptibility assessment
5	Rainfall map	2012; 1:250,000	Rainfall susceptibility assessment
6	GPS field observations	Field survey	Geographical positioning and verification
7	Digital photographs	Field survey	Land-cover verification

The research employed ArcGIS 10.1 for spatial processing and overlay analysis, ENVI 5.1 for satellite image processing and classification, and a Garmin 76CSx handheld GPS receiver for field observations.

2.3. Landsat 8 Image Pre-processing

Landsat 8 image processing involved several stages to prepare the satellite imagery for land-cover classification. Initially, the spectral bands were combined to generate a composite image, followed by image enhancement to improve visual interpretation. Two Landsat 8 image scenes were then mosaicked using the Mosaic to New Raster function in ArcGIS 10.1 to obtain continuous coverage of the study area. Geometric correction was subsequently performed using 11 Ground Control Points (GCPs), with geographical coordinates collected directly in the field using GPS. The corrected imagery was referenced to the WGS 1984 Universal Transverse Mercator (UTM) coordinate system, Zone 51 South. Finally, the image was clipped using the administrative boundary of Timor Tengah Selatan Regency to obtain the required spatial extent.

2.4. Supervised Land-cover Classification

Land-cover classification was conducted using a supervised classification approach in ENVI 5.1. Training samples were selected by delineating Regions of Interest (ROIs) representing the land-cover characteristics visible in the Landsat 8 imagery. The Maximum Likelihood algorithm was subsequently applied to classify image pixels according to their spectral characteristics and the statistical properties of the training samples. The classification produced six land-cover categories: water bodies, agricultural areas, non-agricultural areas, settlements, bare land, and cloud cover. The classified image was then converted into a spatial dataset for integration with the other thematic parameters.

2.5. Classification Accuracy Assessment and Field Verification

The land-cover classification was evaluated using a confusion matrix to examine the correspondence between classified categories and reference information. The original research reported an overall classification accuracy of 96.07%. In addition, field verification was conducted at selected locations using a Garmin 76CSx handheld GPS receiver and digital photographs. The field observations were used to examine the actual land-cover conditions and support corrections to the classification results. The overall accuracy reflects land-cover classification, not the final susceptibility map.

2.6. Thematic Parameter Classification and Scoring

Landslide susceptibility assessment involved four environmental parameters: slope gradient, soil type, rainfall, and land cover. Each parameter was represented by a thematic spatial layer and assigned a numerical score according to the criteria documented in the original research. Slope gradients were classified into five categories, ranging from 0–8% to greater than 40%. Soil types were also grouped into five susceptibility categories, with scores ranging from 10 to 50. Land-cover and rainfall scores were obtained from the thematic attribute data used in the original spatial analysis.

Table 2. Slope and soil-type scoring criteria

Parameter	Classification	Score
Slope	0–8%	10
	8–15%	20
	15–25%	30
	25–40%	40
	>40%	50
Soil type	Alluvial, Glei, Grey Hydromorphic, Groundwater Laterite	10
	Latosol, District Latosol, Eutric Latosol, Humic Latosol	20
	Brown Forest Soil, Non-calcic, District Cambisol, Eutric Cambisol, Ustic Cambisol	30
	Andosol, Lateritic Grumusol, Podsolic	40
	Regosol, Lithosol, Mediteran, Organosol, Renzina	50

Table 3. Land-cover and rainfall scoring criteria

Parameter	Classification / spatial attribute	Score
Land cover	Non-agricultural areas	10
	Agricultural areas	20
	Settlements	30
	Water bodies	40
	Bare land	50
Rainfall	Spatial attribute records assigned to score 40	40
	Spatial attribute records assigned to score 50	50

The rainfall scores were based on the spatial attribute records of the original thematic map. The original classification table contains multiple rainfall ranges assigned to these two scores. These ranges should be retained in the supplementary dataset to ensure reproducibility.

2.7. Spatial Database Development and GIS Overlay Analysis

The thematic datasets were processed through spatial editing, topology construction, and spatial database development in ArcGIS 10.1. Attribute information representing soil type, slope, rainfall, and land cover was integrated with the corresponding spatial layers through attribute joining. The resulting spatial database was used to support the subsequent analysis. GIS overlay analysis was then conducted by integrating the four environmental parameters within the administrative boundary of Timor Tengah Selatan Regency. The total susceptibility score was calculated by summing the individual scores assigned to each parameter, as expressed in Equation (1).

$$S_{\text{total}} = S_{\text{land cover}} + S_{\text{slope}} + S_{\text{soil}} + S_{\text{rainfall}} \qquad \ldots(1)$$

The total scores were subsequently classified into five landslide susceptibility categories using the classification intervals reported in the original research.

Table 4. Landslide susceptibility classification based on total scores

No.	Total score	Susceptibility category
1	39–71	Not susceptible
2	72–104	Low
3	105–137	Moderate
4	138–170	High
5	171–203	Very high

The final susceptibility map represented the spatial distribution of the five categories across Timor Tengah Selatan Regency. This map was used to identify geographical areas with different levels of potential landslide susceptibility.

3. RESULTS AND DISCUSSION

3.1. Landsat 8 Image Processing and Land-Cover Classification

The Landsat 8 imagery used in this study was processed to obtain land-cover information for South Central Timor Regency, East Nusa Tenggara, Indonesia. The image-processing stages included geometric correction, image cropping, training sample selection, and supervised classification. Geometric correction was performed using the georeferencing technique in ArcGIS 10.1, while image classification was conducted using ENVI 5.1. The supervised classification approach employed the Maximum Likelihood algorithm. Training samples were selected through Regions of Interest to represent the spectral characteristics of the land-cover classes. Based on the classification results, six land-cover classes were identified: water bodies, agricultural areas, non-agricultural areas, settlements, bare land, and cloud cover. The classification results are presented in Figure 1.

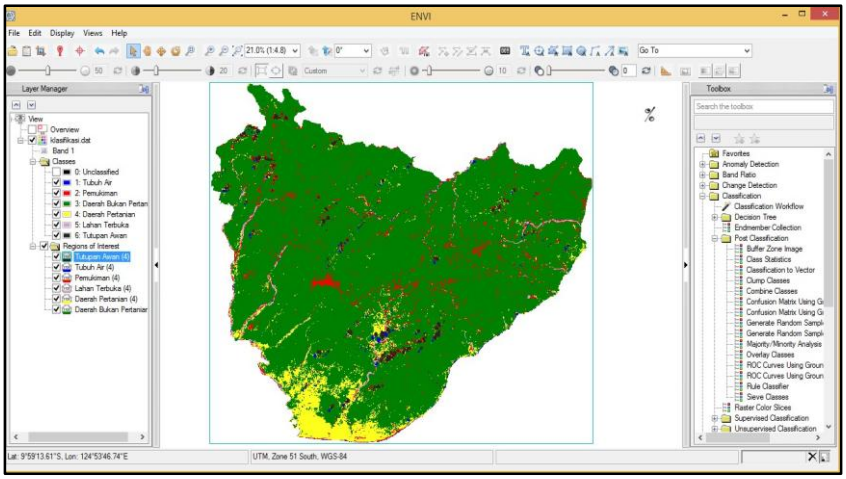


Figure 1. Landsat 8 Land-Cover Classification Map of South Central Timor Regency

The resulting land-cover map was subsequently used as one of the spatial parameters in the landslide susceptibility analysis. The classification provided information on the distribution of different land-cover conditions within the study area.

3.2. Field Verification and Classification Accuracy

Field verification was conducted to evaluate the consistency of the Landsat 8 land-cover classification with actual land-cover conditions. Eight selected locations were checked using geographical coordinates and field observations. The verification process focused on locations considered uncertain during the classification process.The eight verification points represented several land-cover categories, including settlements, agricultural areas, non-agricultural areas, water bodies, and bare land.

Table 1. Field Verification of Landsat 8 Land-Cover Classification

Point	Easting	Northing	Classified land cover	Verified land cover
1	637718	8909418	Settlement	Settlement
2	625315	8903181	Agricultural area	Agricultural area
3	636552	8884603	Agricultural area	Agricultural area
4	660975	8931977	Non-agricultural area	Non-agricultural area
5	673358	8935589*	Water body	Water body
6	670691	8895375	Non-agricultural area	Non-agricultural area
7	692122	8918989	Settlement	Settlement
8	694021	8923059	Bare land	Bare land

Note: The fifth coordinate is reproduced from the original verification table; the thesis narrative contains a different Northing value. This coordinate should be checked against the original GPS record.

The distribution of the eight field verification points is presented in Figure 2.

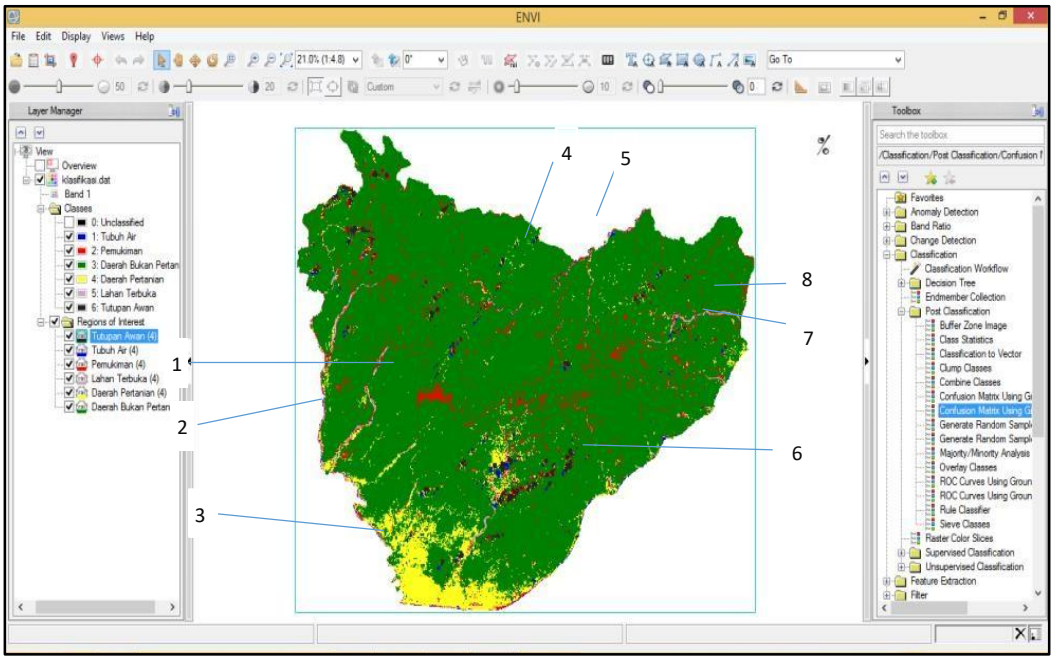


Figure 2. Distribution of Field Verification Points for Land-Cover Classification

The classification accuracy was evaluated using a confusion matrix. The thesis reports 368,959 correctly classified observations out of 384,042 total observations. The resulting accuracy was calculated as follows:

$$Accuracy = \frac{368959}{384042} \times 100\%$$

$$Accuracy = 96.0726\%$$

Thus, the land-cover classification achieved an overall accuracy of 96.0726%. This result indicates a high level of agreement between the classification results and the reference data used in the study.

Table 2. Summary of Land-Cover Classification Accuracy

Accuracy component	Number
Correctly classified observations	368,959
Total observations	384,042
Overall accuracy	96.0726%

The accuracy value refers specifically to the Landsat 8 land-cover classification and does not represent an independent validation of the final landslide susceptibility map.

3.3. Spatial Parameters for Landslide Susceptibility Identification

The identification of potentially landslide-prone areas involved four environmental parameters: land cover, rainfall, slope, and soil type. These parameters were represented as thematic maps and subsequently integrated through spatial overlay analysis.

3.3.1. Land-Cover Parameter

The land-cover map was derived from the Landsat 8 supervised classification. Six classes were identified: water bodies, agricultural areas, non-agricultural areas, settlements, bare land, and cloud cover. The classified land-cover information was integrated with the administrative boundary map to identify the spatial distribution of land-cover categories within the regency.

3.3.2. Rainfall Parameter

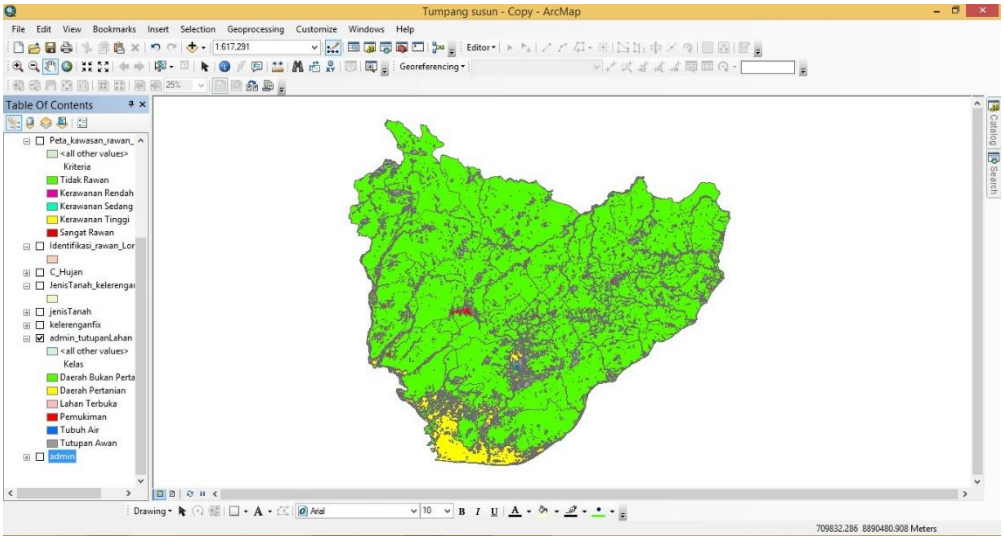
The rainfall map was used to represent the spatial distribution of rainfall conditions across the study area. This parameter was included in the analysis because rainfall is one of the environmental factors considered in the identification of landslide-prone areas.

3.3.3. Slope Parameter

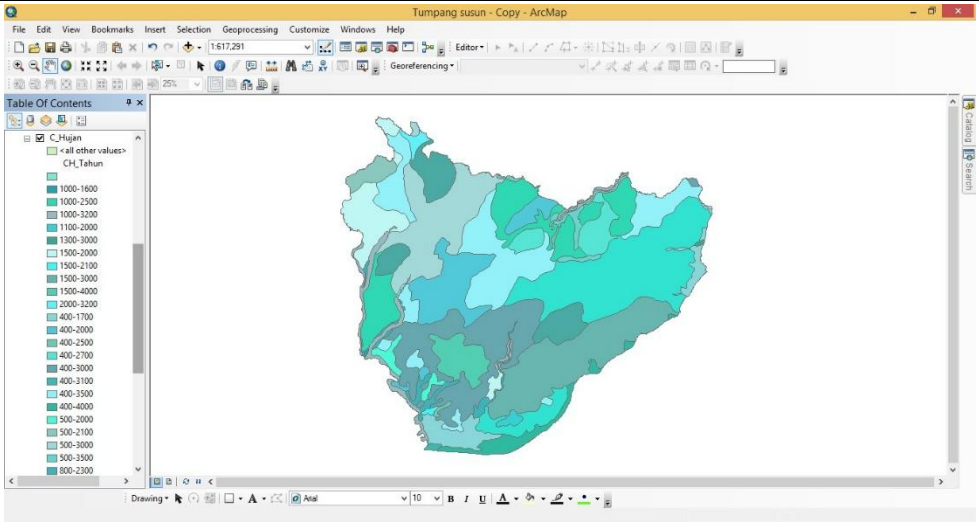
The slope map was used to represent variations in terrain steepness. The study identified slopes exceeding 40% as one of the characteristics associated with very high landslide susceptibility. In contrast, slopes ranging from 0–8% were associated with lower susceptibility.

3.3.4. Soil-Type Parameter

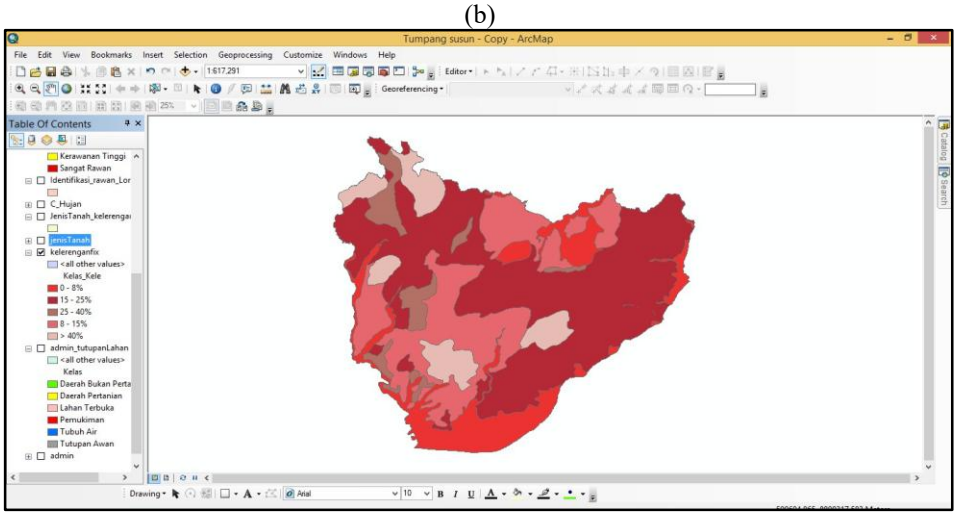
The soil-type map was included to represent the distribution of soil characteristics within the study area. The thesis identifies Renzina and District Cambisol soil types among the characteristics associated with very high susceptibility, while alluvial soils are associated with lower susceptibility. The four spatial parameters were then prepared for integration through the overlay process.



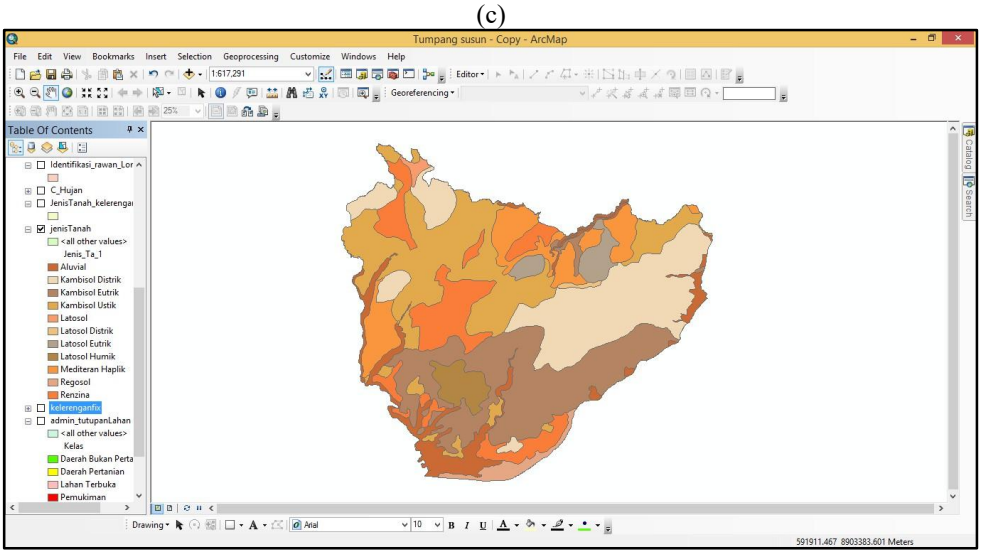
(a)



(b)



(c)



(d)

Figure 3. Spatial Parameters Used in Landslide Susceptibility Analysis

The original thematic maps should be arranged as a four-panel figure:

- (a) Land-cover map.
- (b) Rainfall map.
- (c) Slope map.
- (d) Soil-type map.

3.4. Spatial Overlay and Landslide Susceptibility Scoring

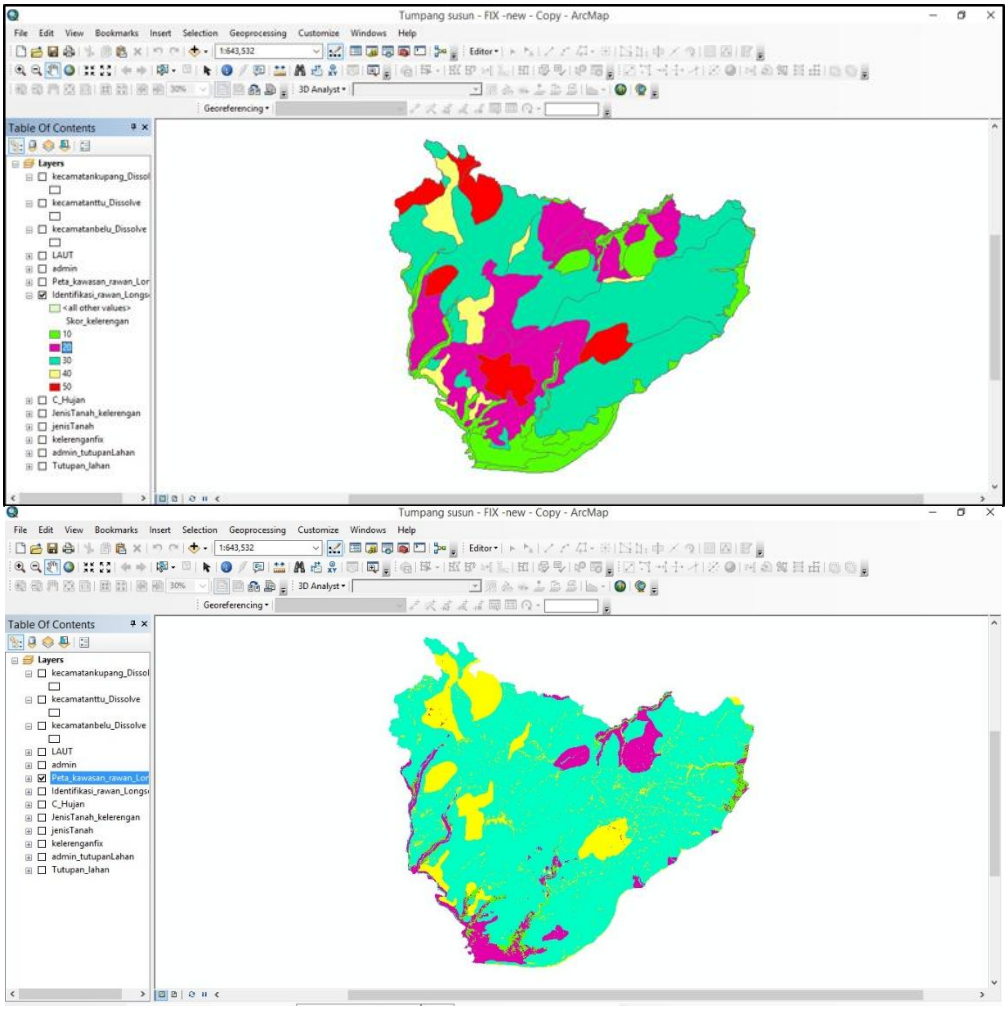
The four environmental parameters were integrated through a spatial overlay process. The overlay involved the administrative boundary map, land-cover map, soil-type map, rainfall map, and slope map. The process was conducted sequentially to produce an integrated spatial dataset for landslide susceptibility identification. The scores assigned to the four parameters were combined to obtain the total susceptibility score for each spatial unit.

The total score was subsequently classified into five susceptibility categories. The resulting score intervals are presented in Table 3.

Table 3. Landslide Susceptibility Classes Based on Total Scores

No.	Susceptibility class	Total score
1	Not susceptible	39–71
2	Low susceptibility	72–104
3	Moderate susceptibility	105–137
4	High susceptibility	138–170
5	Very high susceptibility	171–203

The classification results were used to distinguish areas with different levels of landslide susceptibility. The five classes were then represented spatially through the final susceptibility map.



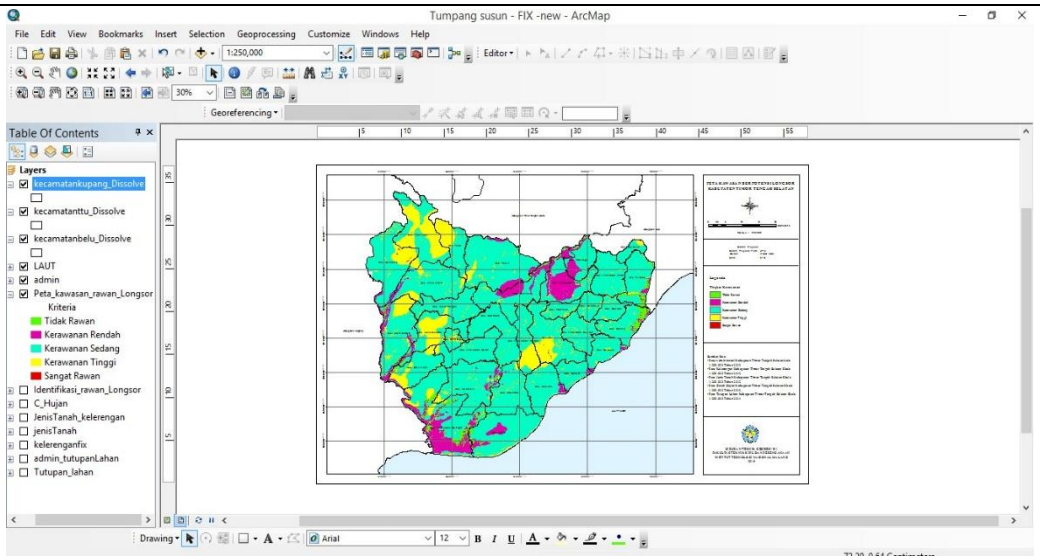


Figure 4. Spatial Overlay Results for Landslide Susceptibility Identification

3.5. Spatial Distribution of Landslide Susceptibility

The final overlay analysis identified five landslide susceptibility classes across South Central Timor Regency. The resulting distribution indicates that moderate susceptibility is the dominant class, while very high susceptibility occupies the smallest area.

Table 4. Area Distribution of Landslide Susceptibility Classes

Susceptibility class	Area (ha)	Percentage (%)
Not susceptible	8,229.700	2.08
Low susceptibility	38,851.323	9.84
Moderate susceptibility	293,501.038	74.35
High susceptibility	53,978.392	13.67
Very high susceptibility	198.596	0.05
Total	394,759.049	100.00

The moderate susceptibility class covered 293,501.038 ha, equivalent to 74.35% of the total study area. The high susceptibility class accounted for 53,978.392 ha (13.67%), while the low susceptibility class covered 38,851.323 ha (9.84%). Areas classified as not susceptible covered 8,229.700 ha (2.08%). Meanwhile, the very high susceptibility class represented the smallest area, covering 198.596 ha (0.05%). The final spatial distribution is presented in Figure 5.

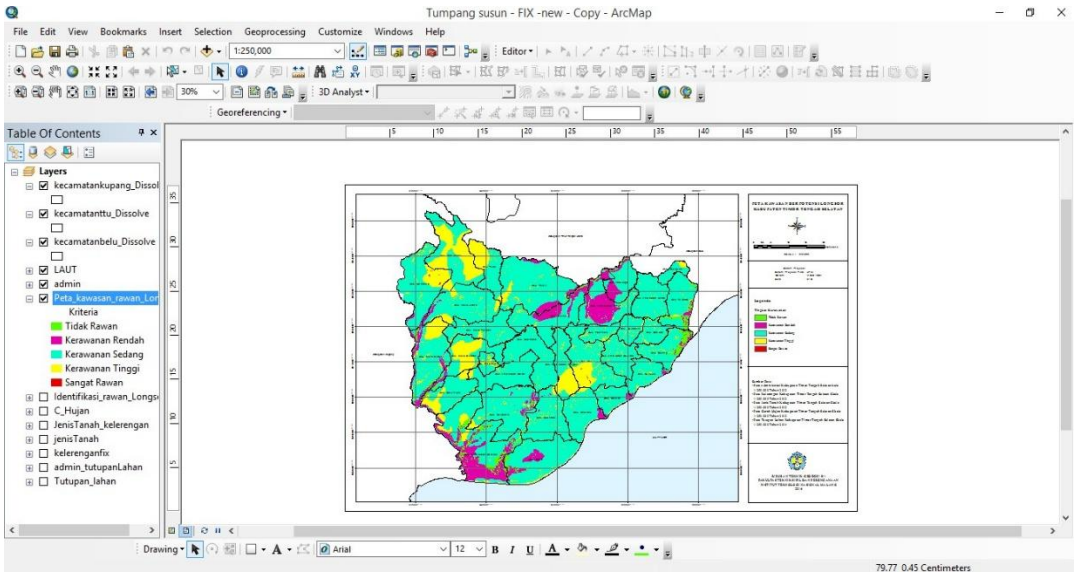


Figure 5. Final Landslide Susceptibility Map of South Central Timor Regency

The final map shows the spatial variation of susceptibility classes across the regency. The distribution indicates that moderate susceptibility is widespread, whereas very high susceptibility occurs in relatively limited locations.

3.6. Environmental Characteristics of Landslide Susceptibility

The spatial analysis also indicates relationships between the environmental characteristics and the resulting susceptibility classes. Areas characterized by slopes exceeding 40%, high rainfall, Renzina and District Cambisol soils, and settlement land cover tend to fall within the very high susceptibility category. In contrast, areas with slopes ranging from 0–8%, low rainfall, alluvial soil types, and non-agricultural land cover tend to be associated with low susceptibility. These findings demonstrate that the susceptibility classification reflects the combined spatial characteristics of the four parameters. The resulting categories should therefore be interpreted as outcomes of the integrated scoring and overlay process rather than the effect of a single environmental parameter.

3.7. District-Level Distribution of Landslide Susceptibility

The district-level analysis provides more detailed information regarding the distribution of landslide susceptibility across the 32 districts included in the original study. The results show that susceptibility classes vary between districts. Some districts contain all five classes, while others are dominated by moderate and high susceptibility categories.

Table 5. District-Level Distribution of Landslide Susceptibility Areas
Area values in hectares. A dash (—) means that the original thesis states that the class is absent or does not provide an area for that class.

District	Not susceptible	Low	Moderate	High	Very high
Amanuban Barat	7.716*	21.147*	10,731.594	541.355	—
Amanuban Selatan	3,099.547	9,661.380	8,585.896	2,347.448	11.429
Amanuban Tengah	—	—	5,739.404	3,558.922	—
Amanuban Timur	240.329	6,520.391	6,803.473	503.556	—
Amanatun Selatan	—	—	7,798.350	679.354	—
Amanatun Utara	—	—	10,295.788	389.540	—
Batu Putih	143.581	357.755	7,455.504	2,614.310	10.871
Boking	1,440.575	775.265	6,739.143	503.323	—
Fatukopa	190.386	2,011.355	5,405.625	111.085	16.735
Fatumnasi	—	—	9,414.302	9,806.363	8.614
Fautmolo	—	—	3,739.196	503.868	—
Ki’e	—	—	11,933.410	4,471.385	45.912
Kok’baun	—	—	2,515.069	339.513	—
Kolbano	—	422.382	9,851.141	720.846	—
Kot’olin	—	271.050	5,319.471	210.707	—
Kota So’e	—	2,140.404	678.434	210.707	—
Kualin	600.165	2,018.040	16,241.312	691.236	—
Kuanfatu	138.133	126.644	12,525.837	740.706	1.009
Kuatnana	40.346	14.097	13,566.603	441.407	0.103
Mollo Selatan	191.534	495.274	6,485.101	5,158.929	—
Mollo Tengah	—	3.207	10,299.106	769.169	—
Mollo Barat	490.692	2,052.864	12,160.193	3,726.890	7.140
Mollo Utara	—	480.464	14,743.217	2,085.851	0.445
Noebana	—	—	4,143.800	457.043	—
Noebeba	238.099	913.943	16,987.872	1,082.647	4.639
Nunbena	—	438.463	14,709.015	3,807.200	78.059
Nunkolo	—	241.111	6,245.955	463.748	—
Oenino	232.394	3,016.173	11,452.294	553.259	—
Polen	40.783	1,821.493	22,145.616	1,595.751	13.640
Santian	—	—	4,451.877	523.895	—
Tobu	—	—	5,506.656	3,798.191	—
Toianas	1,135.420	427.463	8,830.784	570.188	—

3.7.1. Comparison of Selected Districts

The district-level results illustrate differences in susceptibility distribution. In Amanuban Selatan, all five susceptibility classes were identified. Moderate susceptibility covered 8,585.896 ha, while low susceptibility

accounted for 9,661.380 ha. The very high susceptibility class occupied 11.429 ha. In Amanuban Tengah, the analysis identified only moderate and high susceptibility areas, covering 5,739.404 ha and 3,558.922 ha, respectively. No areas were reported in the not susceptible, low, or very high susceptibility classes.

Fatumnasi showed a different pattern, with 9,806.363 ha classified as high susceptibility and 9,414.302 ha classified as moderate susceptibility. This indicates that high susceptibility occupied a substantial area in this district. In contrast, Kualin was dominated by moderate susceptibility, covering 16,241.312 ha. The district also contained 2,018.040 ha of low susceptibility and 691.236 ha of high susceptibility.

Polen recorded the largest moderate susceptibility area among the district examples presented, at 22,145.616 ha. This was followed by Noebeba, with 16,987.872 ha, and Kualin, with 16,241.312 ha. These district-level findings indicate that although moderate susceptibility dominates at the regency level, the distribution of high and very high susceptibility varies considerably between districts.

3.8. Overall Distribution of Landslide Susceptibility

The overall distribution of susceptibility classes is summarized in Figure 6. The graph illustrates the substantial difference between the moderate susceptibility class and the other four classes.

Landslide susceptibility area distribution. Area of each susceptibility class in South Central Timor Regency.

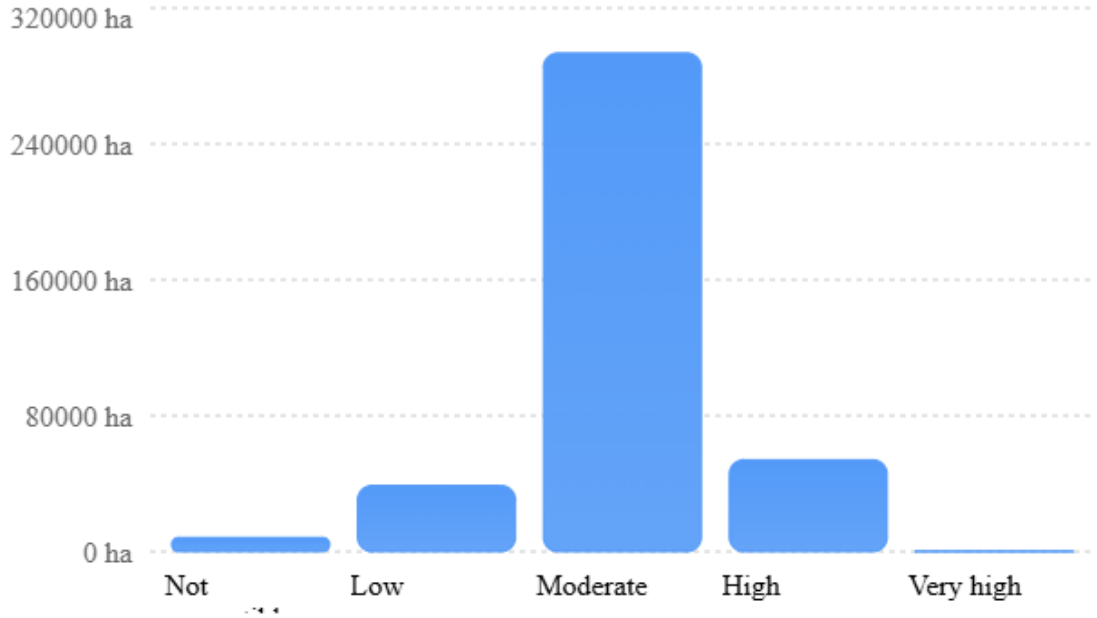


Figure 6. Area Distribution of Landslide Susceptibility Classes in South Central Timor Regency

The graph confirms that moderate susceptibility is the dominant category, covering approximately three-quarters of the total study area. High susceptibility represents the second-largest category, followed by low susceptibility. The very high susceptibility class occupies the smallest area.

This distribution provides an overview of the spatial pattern of potential landslide susceptibility in the study region and complements the information presented in the final susceptibility map.

The findings demonstrate that the integration of Landsat 8 imagery and Geographic Information Systems (GIS) provides a practical approach for identifying areas with different levels of landslide susceptibility in South Central Timor Regency. The analysis combines four environmental parameters, namely land cover, rainfall, slope, and soil type, through a thematic map overlay process. This integration is important because landslide susceptibility is not determined by a single environmental condition but is associated with the interaction of terrain characteristics, geological conditions, rainfall, and land-surface characteristics. The resulting classification identifies five susceptibility categories, ranging from not susceptible to very high susceptibility, providing a spatial representation of the variation in environmental conditions across the study area.

One of the most important findings is the dominance of the moderate susceptibility class, which covers 293,501.038 ha or 74.35% of the total study area. The high susceptibility class covers 53,978.392 ha (13.67%), while low susceptibility accounts for 38,851.323 ha (9.84%). Areas classified as not susceptible cover 8,229.700 ha (2.08%), and very high susceptibility areas account for only 198.596 ha (0.05%). This distribution indicates that most of the study area falls within an intermediate susceptibility category. However, the relatively small extent of the very high susceptibility class should not be interpreted as evidence that landslide hazards are insignificant. Rather, it indicates that locations with the most unfavorable combination of the four assessed parameters are spatially limited according to the scoring model used in this research.

The environmental characteristics identified in the study provide further insight into this spatial pattern. Areas with slopes exceeding 40%, high rainfall, Renzina and District Cambisol soil types, and settlement land cover tend to be associated with very high susceptibility scores. Conversely, areas with slopes ranging from 0–8%, low rainfall, alluvial soils, and non-agricultural land cover tend to be associated with lower susceptibility scores. These findings suggest that the combined environmental conditions influence the final classification. Nevertheless, the results should be interpreted as spatial associations generated by the scoring and overlay procedure, rather than as proof of direct causal relationships between individual parameters and landslide occurrence.

Another important finding is the variation in susceptibility distribution among the 32 districts. For example, Amanuban Selatan contains all five susceptibility classes, whereas Amanuban Tengah is characterized by moderate and high susceptibility classes in the reported results. Fatumnasi also exhibits a substantial extent of high susceptibility, covering 9,806.363 ha, compared with 9,414.302 ha of moderate susceptibility. These differences demonstrate that a regency-level summary alone cannot fully represent the spatial characteristics of landslide susceptibility. District-level information is therefore necessary to identify areas requiring more detailed investigation and differentiated land-use management.

The land-cover classification achieved an overall accuracy of 96.0726%, indicating a high level of agreement between the classified image and the reference observations used in the study. However, this accuracy value specifically evaluates the Landsat 8 land-cover classification. It does not demonstrate the predictive accuracy of the final landslide susceptibility map. Consequently, the main strength of the present study lies in its integration of remote sensing and GIS to produce spatially explicit susceptibility information, while the reliability of the final susceptibility classification still requires independent validation using a landslide inventory or field evidence of actual landslide occurrences.

The findings of this study are consistent with previous research demonstrating the importance of integrating multiple environmental parameters in GIS-based landslide susceptibility mapping. Devara et al. [29], for example, developed landslide susceptibility maps by integrating multi-temporal InSAR observations and the Analytical Hierarchy Process (AHP) within a GIS-based multi-criteria decision analysis framework. Their study emphasizes the importance of combining terrain-derived variables and other thematic information to represent spatial differences in landslide susceptibility. Similarly, the present study integrates land cover, rainfall, slope, and soil type through thematic map overlay. Although the analytical approaches differ, both studies demonstrate the usefulness of GIS for combining multiple sources of spatial information to identify potentially unstable areas.

The present findings also correspond with the broader research trends discussed by Lima et al. [30], who reviewed 2,585 publications on data-driven landslide susceptibility assessment. Their review identified slope angle, aspect, and geological characteristics as frequently used conditioning factors in susceptibility mapping. This supports the inclusion of slope and soil-related information in the present study. Nevertheless, the current research uses a relatively straightforward scoring and overlay approach rather than statistical or machine-learning-based modeling. Therefore, its contribution is primarily related to the regional application and spatial integration of environmental data, rather than the development of a new predictive algorithm.

A similar methodological comparison can be made with the work of Tehrani et al. [39], who examined the development and application of machine learning methods in landslide detection, mapping, and susceptibility forecasting. Their review explains that machine learning techniques can identify complex relationships within large environmental datasets, but also highlights challenges related to data availability, model evaluation, and generalization. In comparison, the present study employs a transparent thematic scoring and overlay procedure that allows the contribution of the selected environmental parameters to be represented through spatial classes. This approach is relatively accessible for regional planning applications, particularly where detailed landslide inventories and computational resources for advanced predictive modeling are limited. However, it does not provide the same statistical predictive evaluation as a model trained and tested using an independent landslide inventory.

Further comparison can be drawn from Zhang et al. [40], who evaluated support vector machine, kernel logistic regression, and a deep-learning-based LSNet model for landslide susceptibility mapping in Hanyin County, China. Their study used an inventory of 259 landslides and divided the samples into training and validation datasets. The authors reported that LSNet achieved an accuracy of 0.950 and an area under the receiver operating characteristic curve (AUC) of 0.941. This approach differs from the present study, which classifies susceptibility through the combination of four thematic parameters and does not report an independent validation of the final susceptibility map. The comparison highlights an important methodological distinction: spatial overlay is useful for producing interpretable regional susceptibility classifications, whereas inventory-based machine learning provides additional opportunities to evaluate predictive performance.

The findings are also relevant to the research of Sharma et al. [32], who developed a high-resolution landslide susceptibility mapping framework for India using ensemble machine learning and geospatial big data. Their research emphasizes the importance of data quality, spatial resolution, and ensemble modeling in reducing uncertainty in susceptibility mapping. Compared with their national-scale, high-resolution framework, the present

study focuses on a specific regency and uses Landsat 8 imagery with a spatial resolution of 30 m, together with supporting thematic maps. Although the spatial scales and analytical methods differ, both studies demonstrate the value of geospatial data integration for identifying the spatial distribution of landslide susceptibility. The comparison also suggests opportunities for future improvements through higher-resolution spatial data and more advanced analytical approaches.

Finally, the present study is consistent with the findings of the comparison conducted by Gudiyangada Nachappaet al. [41] on per-pixel and object-based approaches to landslide susceptibility mapping. Their research used ten conditioning factors and independent training and validation inventories, demonstrating that the spatial representation and analytical unit can influence susceptibility mapping performance. This reinforces the importance of considering the scale and spatial structure of the input data when interpreting the susceptibility classes generated in South Central Timor Regency.

Overall, the comparison indicates that the present research shares the general principle of integrating multiple environmental conditioning factors with previous landslide susceptibility studies. Its principal methodological distinction is the use of Landsat 8-derived land-cover information combined with three supporting thematic parameters through a GIS-based scoring and overlay process at the regency and district levels.

The novelty of this research lies primarily in its regional application and the integration of Landsat 8-derived land-cover information with rainfall, slope, and soil-type data to identify landslide susceptibility across South Central Timor Regency. Rather than proposing a new classification algorithm or a new landslide prediction model, the study demonstrates how satellite imagery and GIS can be combined to produce a spatially differentiated susceptibility assessment at both regency and district levels. The use of six land-cover classes derived from Landsat 8 imagery provides an important spatial information layer that is integrated with three additional environmental parameters to generate five susceptibility categories.

A further contribution is the presentation of susceptibility information across 32 districts, allowing the regional pattern to be examined beyond the overall regency-level distribution. The finding that moderate susceptibility dominates 74.35% of the study area, while the extent of high and very high susceptibility varies among districts, provides a more detailed spatial basis for identifying locations that may require further investigation. This district-level perspective is particularly relevant because regional susceptibility patterns may conceal substantial differences between individual administrative areas.

Therefore, the novelty should be understood as an applied and spatial-contextual contribution: the study provides an integrated geospatial assessment of landslide susceptibility for South Central Timor Regency using Landsat 8 and GIS. It does not claim methodological novelty in the Maximum Likelihood classification or thematic overlay techniques, which have already been widely used in remote sensing and landslide susceptibility research.

The findings have several implications for regional spatial planning, disaster mitigation, and the management of environmental information. First, the landslide susceptibility map can serve as an initial spatial reference for local government agencies in identifying districts and locations that require more detailed geological, geotechnical, and field investigations. The identification of high and very high susceptibility areas is particularly relevant for prioritizing site assessments, monitoring slope conditions, and reviewing land-use activities in areas with unfavorable environmental characteristics.

Second, the district-level results provide information that can support more differentiated planning strategies. Districts with relatively extensive high susceptibility areas, such as Fatumnasi, may require particular attention in subsequent field investigations and land-use evaluations. Meanwhile, the dominance of moderate susceptibility across the regency indicates that mitigation planning should not focus exclusively on the limited very high susceptibility areas. Moderate susceptibility areas should also be considered in broader regional planning, especially where changes in land use, infrastructure development, or rainfall conditions may influence slope stability.

Third, the study demonstrates the practical value of integrating remote sensing and GIS for regional environmental assessment. Landsat 8 imagery provides land-cover information over a relatively extensive area, while GIS facilitates the integration of this information with supporting thematic datasets. This approach can be used as a foundation for developing an updated geospatial database, particularly when combined with more recent satellite imagery, detailed topographic information, and verified landslide occurrence records.

However, the resulting map should be used as a preliminary susceptibility information product rather than as a stand-alone basis for determining disaster risk or issuing early warnings. Susceptibility represents the spatial tendency of an area to experience landslides under certain environmental conditions, whereas risk assessment also requires information about hazard intensity, exposure, vulnerability, and potential consequences. Accordingly, the results are most useful as a supporting instrument for regional screening and prioritization, followed by detailed field-based assessment.

The findings of this study can be generalized primarily to the spatial assessment of landslide susceptibility in areas with environmental and data conditions comparable to those of South Central Timor Regency. The integration of land cover, rainfall, slope, and soil type through GIS-based scoring and overlay can provide a practical framework for other regional studies, particularly where satellite imagery and thematic spatial datasets

are available. Nevertheless, the susceptibility classes and their spatial distribution should not be directly transferred to other regions without considering differences in geological conditions, topography, rainfall patterns, land-cover characteristics, and the quality of available spatial data.

Several limitations should be considered when interpreting the results. First, the land-cover information was derived from Landsat 8 imagery acquired in 2014, with a spatial resolution of 30 m. Consequently, the resulting land-cover classification represents the conditions captured by the imagery at that time and should not be interpreted as a representation of current land-cover conditions in 2026. Changes in settlement expansion, agricultural activities, vegetation cover, and infrastructure development may have altered the spatial characteristics of the study area since the image acquisition period.

Second, the land-cover classification accuracy of 96.0726% was obtained from the confusion matrix and reference observations used in the original study. Although this result indicates strong agreement for land-cover classification, it does not establish the accuracy of the final landslide susceptibility map. Independent validation using a spatial landslide inventory, field observations of landslide locations, or historical landslide records was not clearly established in the original research. Therefore, the susceptibility classes should be interpreted as the outcomes of a multi-parameter scoring model rather than as statistically validated probabilities of landslide occurrence.

Third, the study used four environmental parameters: land cover, rainfall, slope, and soil type. Although these parameters provide important information for regional susceptibility screening, other factors may also influence landslide processes, including lithology, geological structures, distance to rivers, drainage conditions, aspect, elevation, road construction, and changes in land use. Their exclusion may limit the ability of the model to represent the full complexity of landslide-generating processes.

Fourth, the scoring and overlay approach depends on the classification criteria and scores assigned to each parameter. The resulting susceptibility map is therefore influenced by the selected scoring scheme and class intervals. Different weighting systems, classification methods, or spatial resolutions may produce different susceptibility distributions. Future studies could examine the sensitivity of the results to alternative scoring schemes and compare the current approach with statistical or machine-learning-based models.

Finally, the original study contains some inconsistencies in the reported district-level area values and certain coordinate records. These issues should be checked against the original GIS attribute tables and field records before the district-level figures are used for policy decisions or further quantitative comparison. The total area and district-level summaries should also be reconciled with the administrative boundary dataset used in the analysis.

Considering these limitations, future research should update the land-cover data using more recent satellite imagery, incorporate a verified landslide inventory, expand the range of conditioning factors where reliable data are available, and conduct independent validation of the final susceptibility map. Such improvements would strengthen the reliability, temporal relevance, and transferability of the resulting landslide susceptibility information.

4. CONCLUSION

This study demonstrates the application of Landsat 8 imagery and Geographic Information Systems (GIS) for identifying areas with different levels of landslide susceptibility in South Central Timor Regency, East Nusa Tenggara, Indonesia. The integration of four environmental parameters, namely land cover, rainfall, slope, and soil type, through spatial scoring and overlay analysis successfully identified five susceptibility classes: not susceptible, low, moderate, high, and very high. The results indicate that moderate susceptibility dominates the study area, covering 293,501.038 ha (74.35%), followed by high susceptibility covering 53,978.392 ha (13.67%), low susceptibility covering 38,851.323 ha (9.84%), not susceptible areas covering 8,229.700 ha (2.08%), and very high susceptibility areas covering 198.596 ha (0.05%). The district-level analysis further reveals spatial variations in susceptibility, demonstrating the importance of examining landslide-prone areas at both regency and district scales. Overall, the integration of remote sensing and GIS provides useful spatial information for preliminary identification of potentially landslide-prone areas and can support regional land-use planning and disaster mitigation efforts. Future studies should incorporate more recent satellite imagery, additional environmental conditioning factors, and verified landslide inventory data to improve the temporal relevance and reliability of susceptibility mapping. Independent validation and comparisons with statistical or machine-learning models are also recommended to evaluate the predictive performance and robustness of the resulting susceptibility maps.

ACKNOWLEDGEMENTS

The author would like to express sincere gratitude to all parties who provided support and assistance throughout the research process. Special thanks are extended to the academic supervisors for their valuable guidance, constructive feedback, and encouragement. The author also gratefully acknowledges the relevant

institutions and local authorities in South Central Timor Regency for their assistance in providing data and facilitating field activities. Appreciation is also extended to everyone who contributed, directly or indirectly, to the completion of this research.

REFERENCES

[1] I. Alcántara-Ayala, "Landslides in a changing world," *Landslides*, vol. 22, no. 9, pp. 2851–2865, 2025, doi: 10.1007/s10346-024-02451-1.

[2] M. P. Amarasinghe, S. A. S. Kulathilaka, D. J. Robert, A. Zhou, and H. A. G. Jayathissa, "Risk assessment and management of rainfall-induced landslides in tropical regions: A review," *Nat. Hazards*, vol. 120, no. 3, pp. 2179–2231, 2024, doi: 10.1007/s11069-023-06277-3.

[3] R. Pacheco Quevedo, A. Velastegui-Montoya, N. Montalván-Burbano, F. Morante-Carballo, O. Korup, and C. Daleles Rennó, "Land use and land cover as a conditioning factor in landslide susceptibility: A literature review," *Landslides*, vol. 20, no. 5, pp. 967–982, 2023, doi: 10.1007/s10346-022-02020-4.

[4] S. Pereira, P. P. Santos, J. L. Zêzere, A. O. Tavares, R. A. C. Garcia, and S. C. Oliveira, "A landslide risk index for municipal land use planning in Portugal," *Sci. Total Environ.*, vol. 735, p. 139463, 2020, doi: 10.1016/j.scitotenv.2020.139463.

[5] H. Li and N. A. Samsudin, "A systematic review of landslide research in urban planning worldwide," *Nat. Hazards*, vol. 121, no. 6, pp. 6391–6411, 2025, doi: 10.1007/s11069-024-07064-4.

[6] M. Acosta-Quesada and A. Quesada-Román, "Landslides and flood hazard mapping using geomorphological methods in Santa Ana, Costa Rica," *Int. J. Disaster Risk Reduct.*, vol. 113, p. 104882, 2024, doi: https://doi.org/10.1016/j.ijdrr.2024.104882.

[7] Y. Wang and Y. A. Nanehkaran, "GIS-based fuzzy logic technique for mapping landslide susceptibility analyzing in a coastal soft rock zone," *Nat. Hazards*, vol. 120, no. 12, pp. 10889–10921, 2024, doi: 10.1007/s11069-024-06649-3.

[8] L. Mengstie, A. Nebere, M. Jothimani, and B. Taye, "Landslide susceptibility assessment in Addi Arkay, Ethiopia using GIS, remote sensing, and AHP," *Quat. Sci. Adv.*, vol. 15, p. 100217, 2024, doi: 10.1016/j.qsa.2024.100217.

[9] A. Mohan, A. K. Singh, B. Kumar, and R. Dwivedi, "Review on remote sensing methods for landslide detection using machine and deep learning," *Trans. Emerg. Telecommun. Technol.*, vol. 32, no. 7, p. e3998, Jul. 2021, doi: 10.1002/ett.3998.

[10] Shahfahad *et al.*, "Comparative evaluation of operational land imager sensor on board landsat 8 and landsat 9 for land use land cover mapping over a heterogeneous landscape," *Geocarto Int.*, vol. 38, no. 1, p. 2152496, Dec. 2023, doi: 10.1080/10106049.2022.2152496.

[11] C. Wang *et al.*, "Evaluating satellite hyperspectral (Orbita) and multispectral (Landsat 8 and Sentinel-2) imagery for identifying cotton acreage," *Int. J. Remote Sens.*, vol. 42, no. 11, pp. 4042–4063, Jun. 2021, doi: 10.1080/01431161.2021.1887543.

[12] M. L. Clark, "Comparison of multi-seasonal Landsat 8, Sentinel-2 and hyperspectral images for mapping forest alliances in Northern California," *ISPRS J. Photogramm. Remote Sens.*, vol. 159, pp. 26–40, 2020, doi: 10.1016/j.isprsjprs.2019.11.007.

[13] L. Bopche and P. P. Rege, "Landslide susceptibility mapping: An integrated approach using geographic information value, remote sensing, and weight of evidence method," *Geotech. Geol. Eng.*, vol. 40, no. 6, pp. 2935–2947, 2022, doi: 10.1007/s10706-022-02070-4.

[14] A. S. Patil and S. S. Panhalkar, "Remote sensing and GIS-based landslide susceptibility mapping using LNRF method in part of Western Ghats of India," *Quat. Sci. Adv.*, vol. 11, p. 100095, 2023, doi: 10.1016/j.qsa.2023.100095.

[15] Z. Jia, L. Zhu, M. Guo, Y. Zhang, X. Zhang, and Y. Yin, "Rainfall-induced failure mechanisms of cohesive slopes in deep excavations," *Geotech. Geol. Eng.*, vol. 43, no. 9, p. 495, 2025, doi: 10.1007/s10706-025-03465-9.

[16] Z. Zhang *et al.*, "Effects of changes in soil properties caused by progressive infiltration of rainwater on rainfall-induced landslides," *CATENA*, vol. 233, p. 107475, 2023, doi: 10.1016/j.catena.2023.107475.

[17] A. Kahsay, M. Haile, G. Gebresamuel, M. Mohammed, and C. C. Okolo, "Dynamics of soil properties as impacted by contrasting lithology, slope class, and land use types: A case study in semi-arid highlands of northern Ethiopia," *Environ. Monit. Assess.*, vol. 195, no. 9, p. 1091, 2023, doi: 10.1007/s10661-023-11706-8.

[18] S. Qin, J. Cao, J. Yao, C. Zhang, R. Zhang, and Y. Zhao, "Evaluating the uncertainty in landslide susceptibility prediction: Effect of spatial data variability and evaluation unit choices," *Bull. Eng. Geol. Environ.*, vol. 84, no. 3, p. 158, 2025, doi: 10.1007/s10064-025-04180-8.

[19] T. Xiao, S. Segoni, L. Chen, K. Yin, and N. Casagli, "A step beyond landslide susceptibility maps: A simple method to investigate and explain the different outcomes obtained by different approaches," *Landslides*, vol. 17, no. 3, pp. 627–640, 2020, doi: 10.1007/s10346-019-01299-0.

[20] F. Huang, R. Li, F. Catani, X. Zhou, Z. Zeng, and J. Huang, "Uncertainties in landslide susceptibility prediction: Influence rule of different levels of errors in landslide spatial position," *J. Rock Mech. Geotech. Eng.*, vol. 16, no. 10, pp. 4177–4191, 2024, doi: 10.1016/j.jrmge.2024.02.001.

[21] F. Yulianto, G. Nugroho, G. Aruba Chulafak, and S. Suwarsono, "Improvement in the accuracy of the postclassification of land use and land cover using landsat 8 data based on the majority of segment-based filtering approach," *Sci. World J.*, vol. 2021, no. 1, p. 6658818, Jan. 2021, doi: 10.1155/2021/6658818.

[22] B. Ganesh, S. Vincent, S. Pathan, and S. R. G. Benitez, "Utilizing LANDSAT data and the maximum likelihood classifier for analysing land use patterns in shimoga, karnataka," *J. Phys. Conf. Ser.*, vol. 2571, no. 1, p. 12001, 2023, doi: 10.1088/1742-6596/2571/1/012001.

[23] A. D. Debele and I. Tessema, "Geospatial evaluation of flood susceptibility and vulnerability for sustainable urban planning in Sululta town, Oromia region, Ethiopia: A GIS and remote sensing perspective," *Sci. African*, vol. 30, p. e03070, 2025, doi: 10.1016/j.sciaf.2025.e03070.

[24] M. Rashid *et al.*, "Mitigating soil erosion in arid landscapes: Integrating RUSLE and geospatial analysis for sustainable land management," *Environ. Challenges*, vol. 20, p. 101210, 2025, doi: 10.1016/j.envc.2025.101210.
[25] M. Khatun, A. T. M. S. Hossain, H. M. Sayem, M. Moniruzzaman, Z. Ahmed, and K. R. Rahaman, "Landslide susceptibility mapping using weighted-overlay approach in Rangamati, Bangladesh," *Earth Syst. Environ.*, vol. 7, no. 1, pp. 223–235, 2023, doi: 10.1007/s41748-022-00312-2.
[26] U. Sur, P. Singh, and S. R. Meena, "Landslide susceptibility assessment in a lesser Himalayan road corridor (India) applying fuzzy AHP technique and earth-observation data," *Geomatics, Nat. Hazards Risk*, vol. 11, no. 1, pp. 2176–2209, Jan. 2020, doi: 10.1080/19475705.2020.1836038.
[27] M. Hussain *et al.*, "Data-driven multi-hazard susceptibility and community perceptions assessment using a mixed-methods approach," *J. Environ. Manage.*, vol. 388, p. 126009, 2025, doi: 10.1016/j.jenvman.2025.126009.
[28] Q. B. Pham *et al.*, "A comparison among fuzzy multi-criteria decision making, bivariate, multivariate and machine learning models in landslide susceptibility mapping," *Geomatics, Nat. Hazards Risk*, vol. 12, no. 1, pp. 1741–1777, Jan. 2021, doi: 10.1080/19475705.2021.1944330.
[29] M. Devara, A. Tiwari, and R. Dwivedi, "Landslide susceptibility mapping using MT-InSAR and AHP enabled GIS-based multi-criteria decision analysis," *Geomatics, Nat. Hazards Risk*, vol. 12, no. 1, pp. 675–693, Jan. 2021, doi: 10.1080/19475705.2021.1887939.
[30] P. Lima, S. Steger, T. Glade, and F. G. Murillo-García, "Literature review and bibliometric analysis on data-driven assessment of landslide susceptibility," *J. Mt. Sci.*, vol. 19, no. 6, pp. 1670–1698, 2022, doi: 10.1007/s11629-021-7254-9.
[31] M. B. Ibrahim, Z. Mustaffa, A.-L. Balogun, I. S. Hamonangan Harahap, and M. Ali Khan, "Advanced data mining techniques for landslide susceptibility mapping," *Geomatics, Nat. Hazards Risk*, vol. 12, no. 1, pp. 2430–2461, Jan. 2021, doi: 10.1080/19475705.2021.1960433.
[32] N. Sharma, M. Saharia, and G. V Ramana, "High resolution landslide susceptibility mapping using ensemble machine learning and geospatial big data," *CATENA*, vol. 235, p. 107653, 2024, doi: 10.1016/j.catena.2023.107653.
[33] M. Z. Ali *et al.*, "High-resolution landslide mapping and susceptibility assessment: Landslide temporal variations and vegetation recovery," *Adv. Sp. Res.*, vol. 74, no. 8, pp. 3668–3690, 2024, doi: 10.1016/j.asr.2024.06.048.
[34] M. Ehsan, M. T. Anees, A. F. B. A. Bakar, and A. Ahmed, "A review of geological and triggering factors influencing landslide susceptibility: Artificial intelligence-based trends in mapping and prediction," *Int. J. Environ. Sci. Technol.*, vol. 22, no. 16, pp. 17347–17382, 2025, doi: 10.1007/s13762-025-06741-6.
[35] M. Sholichin, F. Othman, T. B. Prayogo, and S. S. P. Rahardjo, "Assessing Landslide susceptibility and formulating adaptation strategies in the Konto Watershed, East Java, Indonesia," *Int. J. Disaster Risk Reduct.*, vol. 113, p. 104797, 2024, doi: 10.1016/j.ijdrr.2024.104797.
[36] R. Patel and A. Patel, "'Evaluating the impact of climate change on drought risk in semi-arid region using GIS technique,'" *Results Eng.*, vol. 21, p. 101957, 2024, doi: 10.1016/j.rineng.2024.101957.
[37] N. Yaa'cob, Z. N. A. Abd Rashid, N. Tajudin, and M. Kassim, "Landslide possibilities using remote sensing and geographical information system (GIS)," *IOP Conf. Ser. Earth Environ. Sci.*, vol. 540, no. 1, p. 12084, 2020, doi: 10.1088/1755-1315/540/1/012084.
[38] Z. Yang *et al.*, "Visualization analysis of rainfall-induced landslides hazards based on remote sensing and geographic information system-an overview," *Int. J. Digit. Earth*, vol. 16, no. 1, pp. 2374–2402, Oct. 2023, doi: 10.1080/17538947.2023.2229797.
[39] F. S. Tehrani, M. Calvello, Z. Liu, L. Zhang, and S. Lacasse, "Machine learning and landslide studies: Recent advances and applications," *Nat. Hazards*, vol. 114, no. 2, pp. 1197–1245, 2022, doi: 10.1007/s11069-022-05423-7.
[40] T. Zhang *et al.*, "Evaluation of different machine learning models and novel deep learning-based algorithm for landslide susceptibility mapping," *Geosci. Lett.*, vol. 9, no. 1, p. 26, 2022, doi: 10.1186/s40562-022-00236-9.
[41] T. Gudiyangada Nachappa, S. Kienberger, S. R. Meena, D. Hölbling, and T. Blaschke, "Comparison and validation of per-pixel and object-based approaches for landslide susceptibility mapping," *Geomatics, Nat. Hazards Risk*, vol. 11, no. 1, pp. 572–600, Jan. 2020, doi: 10.1080/19475705.2020.1736190.